

Rethinking Chain-of-Thought from the Perspective of Self-Training

Zongqian Wu ^{*1 2} Baoduo Xu ^{*1} Ruochen Cui ¹ Mengmeng Zhan ¹ Xiaofeng Zhu ¹ Lei Feng ²

Abstract

Chain-of-thought (CoT) reasoning has emerged as an effective approach for activating latent capabilities in LLMs. Interestingly, we observe that both CoT reasoning and self-training share the core objective: iteratively leveraging model-generated information to progressively reduce prediction uncertainty. Building on this insight, we propose a novel CoT framework to improve reasoning performance. Our framework integrates two key components: (i) a task-specific prompt module that optimizes the initial reasoning process, and (ii) an adaptive reasoning iteration module that dynamically refines the reasoning process and addresses the limitations of previous CoT approaches, *i.e.*, over-reasoning and high similarity between consecutive reasoning iterations. Extensive experiments demonstrate that the proposed method achieves significant advantages in both performance and computational efficiency. Code: <https://github.com/zongqianwu/ST-COT>.

1. Introduction

Chain-of-thought (CoT) reasoning has attracted significant attention in recent years due to its capacity to unlock the latent potential of large language models (LLMs) (Wei et al., 2022). By requiring LLMs to explicitly outline intermediate reasoning processes before generating final outputs, CoT effectively improves the reliability of inferences, particularly when tackling complex reasoning tasks.

Previous CoT methods in LLMs can be divided into two categories, *i.e.*, zero-shot CoT (Kojima et al., 2022) and few-shot CoT (Wei et al., 2022). Zero-shot CoT methods rely on prompts (*e.g.*, ‘‘Let’s think step by step’’) to guide LLMs to generate intermediate reasoning processes relevant to the given question, thereby facilitating logical inference. In contrast, few-shot CoT methods provide some examples that include intermediate reasoning processes from the dataset,

^{*}Equal contribution ¹University of Electronic Science and Technology of China ²SUTD. Correspondence to: Xiaofeng Zhu <seanzhuxf@gmail.com>, Lei Feng <feng_lei@sutd.edu.sg>.

Under Review.

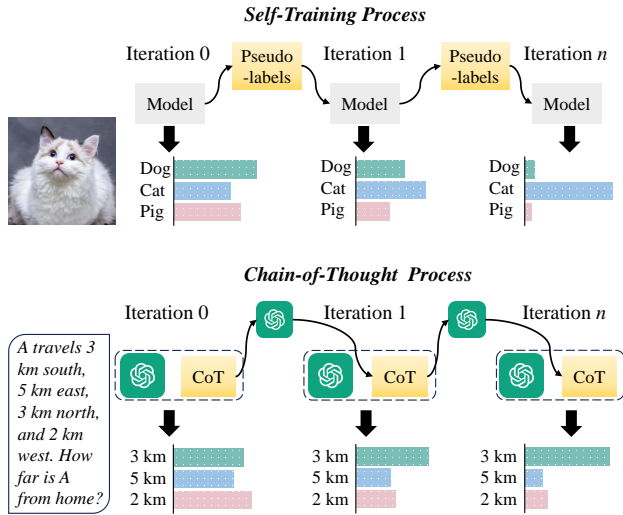


Figure 1. Both self-training and CoT reasoning **iteratively** leverage **model-generated information** (pseudo-labels or reasoning processes) to gradually reduce the uncertainty of predictions.

allowing LLMs to reference these examples during testing to construct reasoning processes. Both zero-shot and few-shot CoT methods leverage the generative capabilities of LLMs to augment question-relevant information, which effectively improves the reliability of inferences. Moreover, this process of information augmentation can be applied iteratively, with deeper iterations enabling LLMs to tackle more complex reasoning tasks (Zhong et al., 2024).

Interestingly, we observe that CoT methods share many conceptual similarities with self-training (a well-established semi-supervised framework), regarding leveraging iteratively model-generated information to enhance task performance (as shown in Figure 1). Concretely, in self-training, pseudo-labels are iteratively generated for unlabeled data and used to retrain the model, thereby progressively enhancing the generalization capabilities of the model. Inspired by this parallel, this paper aims to improve CoT performance from the perspective of self-training.

To this end, we conduct a theoretical analysis of entropy variation in self-training, which demonstrates that the overall uncertainty of predicted samples exhibits a decreasing trend. Furthermore, our experimental results validate that CoT reasoning follows a similar principle, as it iteratively leverages

intermediate reasoning processes to gradually reduce the uncertainty on prediction questions. Based on the insight that CoT reasoning is an uncertainty minimization process, we propose a novel CoT framework to improve reasoning performance, which comprises two main components, *i.e.*, **task-specific prompt** and **adaptive reasoning iteration**. Specifically, the task-specific prompt module is designed to search for optimal prompts with the minimum uncertainty. Unlike generic prompts (*e.g.*, “Let’s think step by step”), our tailored prompt effectively guides LLMs to generate initial reasoning processes aligned with the intrinsic characteristics of the task, significantly reducing the number of iterations required for LLMs to obtain correct answers.

After establishing initial CoT reasoning processes, further iterative refinement can help improve the reasoning process. A straightforward method involves integrating the question, reasoning processes, and output into a new input and reusing the prompt for another reasoning round. However, this intuitive method encounters two key challenges: (i) the correct predictions in earlier iterations may turn incorrect after multiple rounds, a phenomenon we term over-reasoning, and (ii) the reasoning generated in new iterations often closely resembles the previous reasoning. To address these challenges, our adaptive reasoning iteration module is implemented to assess the uncertainty of prediction questions. When the uncertainty is low, the current prediction is adopted as the final output, effectively mitigating challenge (i). However, if uncertainty remains high, the reasoning process continues into the next iteration. In these subsequent iterations, we introduce a new prompt and employ reasoning similarity metrics (*e.g.*, the Jaccard index) to guide LLMs in exploring alternative reasoning pathways. By fostering greater diversity across reasoning iterations, we address the challenge (ii), thereby enhancing the ability of LLMs to tackle complex reasoning tasks effectively.

Our contributions can be summarized as follows:

- Through a combination of theoretical analysis and experimental validation, we reveal that both self-training and CoT reasoning share the core objective of iteratively leveraging model-generated information to gradually reduce the uncertainty of predictions (*i.e.*, entropy minimization), thereby turning some early incorrect predictions into correct ones.
- We design a task-specific prompt module to search for optimal prompts that generate high-quality initial reasoning processes, significantly reducing the number of iterations required for LLMs to obtain correct answers.
- we propose an adaptive reasoning iteration module to dynamically refine the CoT reasoning process and address issues of over-reasoning and high similarity between consecutive reasoning iterations.

2. Understanding Uncertainty in Self-Training and Chain-of-Thought Reasoning

This section investigates the uncertainty in self-training and CoT reasoning by analyzing variations in information entropy and semantic entropy. We observe that while both methods exhibit a general trend of entropy reduction, this pattern does not hold for every data point. Performance improvements are primarily driven by data points where entropy decreases, enabling a transition from incorrect to correct predictions. Specifically, Section 2.1 presents a theoretical analysis of entropy variations in self-training. Building on these insights, Section 2.2 extends the discussion to CoT reasoning, deriving key conclusions that help further enhance the performance of CoT reasoning.

2.1. Information Entropy Variation in Self-Training

The primary objective of self-training is to reduce prediction uncertainty by leveraging pseudo-labels generated by the model, where the uncertainty can be quantified using information entropy. As empirically shown in Figure 8(a) in Appendix, the average entropy of predictions across samples progressively declines throughout the iterative training process. This reduction facilitates some samples being corrected from initial mispredictions to accurate predictions.

However, not all samples exhibit the expected reduction in information entropy. This deviation can be attributed to incorrect annotations within pseudo-labels, which may misdirect the model’s training direction. To provide deeper insights into the entropy variation of self-training, we conducted a theoretical analysis using a Gaussian mixture model. Specifically, an initial classifier with a small yet constant error was constructed and iteratively updated with pseudo-labels based on model predictions. Through this approach, we examined the classifier’s progression from its initial state toward the optimal state, capturing the underlying mechanism of entropy variation. Based on the conclusions of (Frei et al., 2022) regarding the sample complexity of unlabeled samples in self-training, we discover that the intermediate classifier update process is a rotation of the initial classifier towards the Bayes optimal classifier. This conclusion is stated in the following lemma.

Lemma 2.1. *Suppose $(x, y) \sim \mathcal{D}$ where \mathcal{D} is a Gaussian mixture models in $\mathbb{R}^d \times \{\pm 1\}$ with mean μ satisfying $\|\mu\| = \Theta(1)$, *i.e.*, $y \sim \text{Unif}(\{\pm 1\})$ and $x|y \sim \mathcal{N}(y\mu, I)$. Let $\ell(z) = \log(1 + \exp(-z))$, and assume $\sigma \geq \max(1, \|\mu\|)$. Assume we can access a initial classifier β_{init} which satisfies $\Pr_{(x,y) \sim \mathcal{D}}[y \neq \text{sgn}(\beta_{\text{init}}^T x)] = O(1)$. Let $\varepsilon, \delta \in (0, 1)$, and assume that $B = \tilde{\Omega}(\varepsilon^{-1})$, $T = \tilde{\Omega}(d\varepsilon^{-1})$, $\eta = \tilde{\Theta}(d^{-1}\varepsilon)$, suppose θ_t is the angle between β_t and μ , then by running algorithm 1 with step size η and batch size B , when $t < T - 1$, $\theta_t \geq \theta_{t+1}$ holds with probability at least $1 - \delta$, and with probability at least $1 - \delta$, $\theta_{T-1} \leq O(\varepsilon)$.*

Building on Lemma 2.1, assuming that pseudo-labels follow a Bernoulli distribution, and leveraging the relationship between the dot product of the classifier and the samples with θ_t , we can readily derive the entropy variations for different samples and identify the regions to which different types of samples belong, as stated in the following theorem.

Theorem 2.2. *Under the assumptions of Lemma 2.1, let $d = 2$ and suppose $\hat{y}^{(t)}|x \sim \text{Ber}(\vartheta(\beta^T x))$ is the pseudo-label of x , where $\vartheta(z) = \frac{1}{1+e^{-z}}$. Define $l(\alpha)$ as the line $x^T \alpha^\perp = 0$, where α^\perp is perpendicular to α . Let $A(\alpha_1, \alpha_2)$ denote the region swept by $l(\alpha_1)$ rotating to $l(\alpha_2)$ along the trajectory of β_{init} towards μ during self-training. Denote $H_t(x) = \text{Ent}[\hat{y}^{(t)}|x]$ be the entropy of $\hat{y}^{(t)}|x$. For $t < T - 1$, with probability at least $1 - \delta$, the entropy changes as follows: (i) $H_t(x)$ first decreases and then increases if $x \in A(\beta_0, \mu)$; (ii) $H_t(x)$ decreases if $x \in A(\mu, \beta_0^\perp)$; (iii) $H_t(x)$ first increases and then decreases if $x \in A(\beta_0^\perp, \mu^\perp)$; and (iv) $H_t(x)$ increases if $x \in A(\mu^\perp, \beta_0)$.*

Based on Theorem 2.2¹, entropy variation during the iterative process of self-training can be classified into four patterns: (i) a decrease followed by an increase; (ii) a consistent decrease; (iii) a decrease followed by an increase; and (iv) a consistent increase. These patterns are visualized in Figure 2(a), where the light blue, gray, dark blue, and yellow regions correspond to each respective entropy variation pattern. Specifically, we partition \mathbb{R}^2 using vectors $\beta_0, \mu, \beta_0^\perp, \mu^\perp$ and delineate the positions of the initial classifier β_{init} and optimal μ . The updates to the classifier during self-training can be interpreted as the gradual rotation of the initial classifier β_{init} toward the Bayes-optimal classifier μ . Moreover, due to the small initial error of $O(1)$ in the classifier, the angle θ_0 between β_0 and μ is relatively small. As a result, the regions $A(\beta_0, \mu)$ and $A(\beta_0^\perp, \mu^\perp)$ occupy a relatively small proportion of \mathbb{R}^2 , indicating that most samples exhibit monotonic entropy changes.

From experimental and theoretical analyses of self-training, we derive five key insights regarding entropy variation: (i) while the overall entropy of samples typically decreases, this trend does not hold for every individual sample; (ii) most samples exhibit monotonic entropy changes; (iii) the effectiveness of self-training arises from samples undergoing entropy reduction, which enables their transition from incorrect to correct predictions; (iv) in some cases, an increase in entropy could lead to a reversal of predictions, causing previously correct samples to become incorrectly classified; (v) these entropy variations are intrinsically linked to the spatial relationships between the samples and the classifiers β_{init} and μ . These insights will help deepen our understanding of CoT from the perspective of entropy variation.

¹The proofs of the Lemma 2.1 and Theorem 2.2, along with the discussion of Related Work, are provided in Appendix.

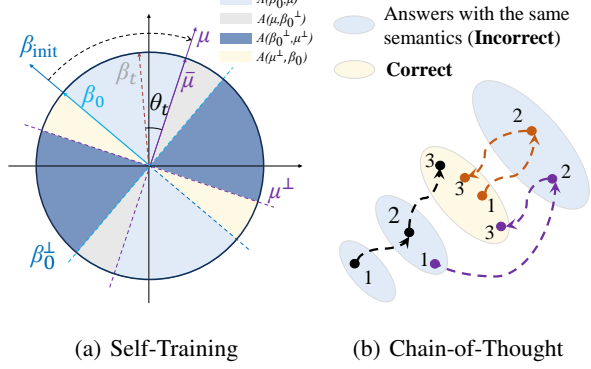


Figure 2. Visualizations of entropy variations in the iterative process of self-training and CoT. In the self-training diagram, the iterative process represents the gradual convergence of the initial classifier β_{init} toward the Bayes optimal classifier μ . At each iteration, changes in the angle between the classifier and the samples in different regions correspond to entropy variations within those samples. In the CoT diagram, the numbers indicate the corresponding iteration rounds. During the first iteration, the reasoning process is guided solely by the prompt, whereas in subsequent iterations, it is jointly influenced by the prompt and the outputs of previous reasoning. Each circle in the diagram represents a set of answers that are semantically equivalent but vary in their expressions. The semantic entropy at each iteration is determined by the distribution of generated answers across different semantic classes.

2.2. Semantic Entropy Variation in Chain-of-Thought

Chain-of-thought (CoT), akin to self-training, relies on model-generated information to enhance task performance. Specifically, CoT aims to reduce the prediction uncertainty in the LLMs by leveraging intermediate reasoning processes generated by the LLMs. This uncertainty can be effectively quantified through the semantic entropy (Farquhar et al., 2024). To formalize this concept, we define the semantic entropy of LLMs with CoT reasoning as follows.

Definition 2.3 (Semantic Entropy of LLMs with CoT Reasoning on a Given Question). Let the set of reasoning processes that an LLMs can generate for a question q and prompt p be denoted as R , with the corresponding set of answers represented as A . Assume that A can be partitioned into disjoint clusters based on semantic equivalence, i.e., $A = \bigcup_{C \in \mathcal{C}} C$, where C is the set of answers with the same semantics. Let $g(C|q, p)$ denote the probability distribution over C . The semantic entropy is then defined as $e = \mathbb{E}_C[-\log g(C|q, p)]$. In practical use, let LLMs generate N distinct answers $\hat{A} = \{a_i\}_{i \in [N]}$, which are then divided into k semantic clusters $\hat{C} = \{C_j\}_{j \in [k]}$. By normalizing, we obtain a discrete probability distribution $\{g_j\}_{j \in [k]}$, where $g_j = |C_j|/N$. Consequently, we can use $\hat{e} = -\sum_{j=1}^k g_j \log g_j$ as an approximation of e .

In self-training, pseudo-labels guide the initial classifier toward the Bayes-optimal classifier. Similarly, in CoT, the reasoning process drives LLMs predictions closer to the cor-

rect answer. Inspired by the analogy between self-training classifiers and LLMs predictions with CoT reasoning, and building on the discussion in Section 2.1, we propose the following definitions for CoT reasoning.

Definition 2.4 (Initial State and the Optimal Answer Group of LLMs with CoT Reasoning on a Given Question). Under the assumptions of Definition 2.3, in $\hat{\mathcal{C}}$, let $j = \arg \max_{i \in [k]} |C_i|$, and define $C_{\text{init}} = C_j$ to represent the initial state in CoT (analogous to the initial classifier in self-training). In \mathcal{C} , define the cluster C_μ containing the correct answer as the optimal state (analogous to the Bayes-optimal classifier in self-training).

To further investigate how semantic entropy evolves within the CoT framework, we propose the following assumption.

Assumption 2.5. As the semantic entropy e decreases, the likelihood of the LLMs with CoT reasoning producing a correct answer to question q increases.

Building on Definitions 2.3 and 2.4, along with Assumption 2.5, the iterative process of applying CoT reasoning to tackle complex questions can be interpreted as LLMs progressively searching for an optimal answer group C_μ , starting from an initial state C_{init} . This process is marked by a gradual reduction in semantic entropy, supported by empirical evidence in Figure 3. The decreasing entropy reflects the refinement of predictions, enabling the correction of initial errors and the generation of accurate answers.

Similar to self-training, not all questions show the expected reduction in semantic entropy during CoT reasoning. This phenomenon may arise from the presence of noisy information in reasoning processes, which could misdirect the reasoning trajectory of LLMs. To verify this, we conducted a simple experiment involving three rounds of iterative CoT reasoning on the AQuA arithmetic dataset, analyzing the semantic entropy variation of LLMs. The results, presented in Figure 8(b) in Appendix, reveal three distinct patterns of semantic entropy variation: (i) monotonic increase or decrease; (ii) increase followed by decrease or decrease followed by increase; (iii) no change. These patterns are visualized in Figure 2(b), where the semantic entropy of each iteration is quantified based on the distribution of the generated answers across different semantic planes. For example, we set the sampling number N of the reasoning process to 3. In the first iteration, the three processes yielded three semantically distinct answers, reflecting a high degree of semantic uncertainty in the LLMs. In the second iteration, the processes converged to two semantically distinct answers, indicating a slight reduction in uncertainty. By the third iteration, all processes arrived at the same semantic answer, reducing the uncertainty to zero. At this stage, the LLMs successfully identified the optimal answer group C_μ . Moreover, the other two patterns of semantic entropy variation in CoT reasoning can also be derived straightforwardly.

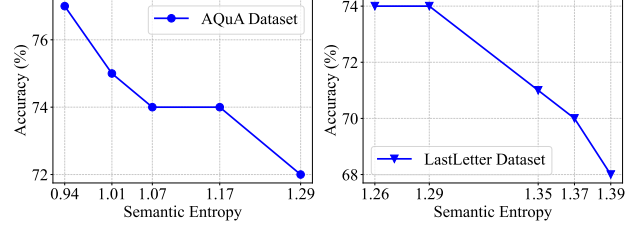


Figure 3. Accuracy under varying levels of semantic entropy on the AQuA and LastLetters datasets (based on 100 sampled instances).

Based on the insights gained from self-training in Section 2.1 and the experimental analysis of CoT reasoning, we derive five important conclusions regarding semantic entropy variations in CoT reasoning: (i) although the overall semantic entropy of questions generally decreases, this trend does not apply to every individual question; (ii) when the reasoning processes of the new iteration are excessively similar to those in the previous iteration, the semantic entropy of certain questions may exhibit no changes; (iii) the effectiveness of CoT reasoning stems from questions undergoing semantic entropy reduction, facilitating a transition from incorrect to correct predictions; (iv) for some questions, an increase in entropy could lead to prediction reversals, where previously correct predictions become incorrect; (v) these variations in semantic entropy are tied to the spatial relationships between the initial state and the optimal answer group of the LLMs with CoT reasoning on a given question.

We will demonstrate in the next section how these findings can be utilized to further enhance CoT performance.

3. The Proposed CoT Framework

Building on the conclusions from the analysis of semantic entropy variation in CoT reasoning presented in Section 2.2, we propose a novel CoT framework to improve reasoning performance. Specifically, we design a task-specific prompt module in Section 3.1 to guide the LLMs in generating high-quality initial reasoning processes. Next, in Section 3.2, we introduce an adaptive reasoning iteration module to refine the reasoning process and address the limitations of traditional CoT approaches, *i.e.*, over-reasoning and excessive similarity between consecutive reasoning iterations. An overview of our proposed CoT framework is provided in Figure 4. Detailed information about the task-specific prompt module is provided in Figure 6 in Appendix.

3.1. Task-Specific Prompt

The conclusion (v) presented in Section 2.2 underscores the pivotal role of CoT reasoning quality in the initial iteration. A high-quality initial CoT reasoning process effectively reduces the distance between the initial state and the optimal answer group, thereby decreasing the number of iterations

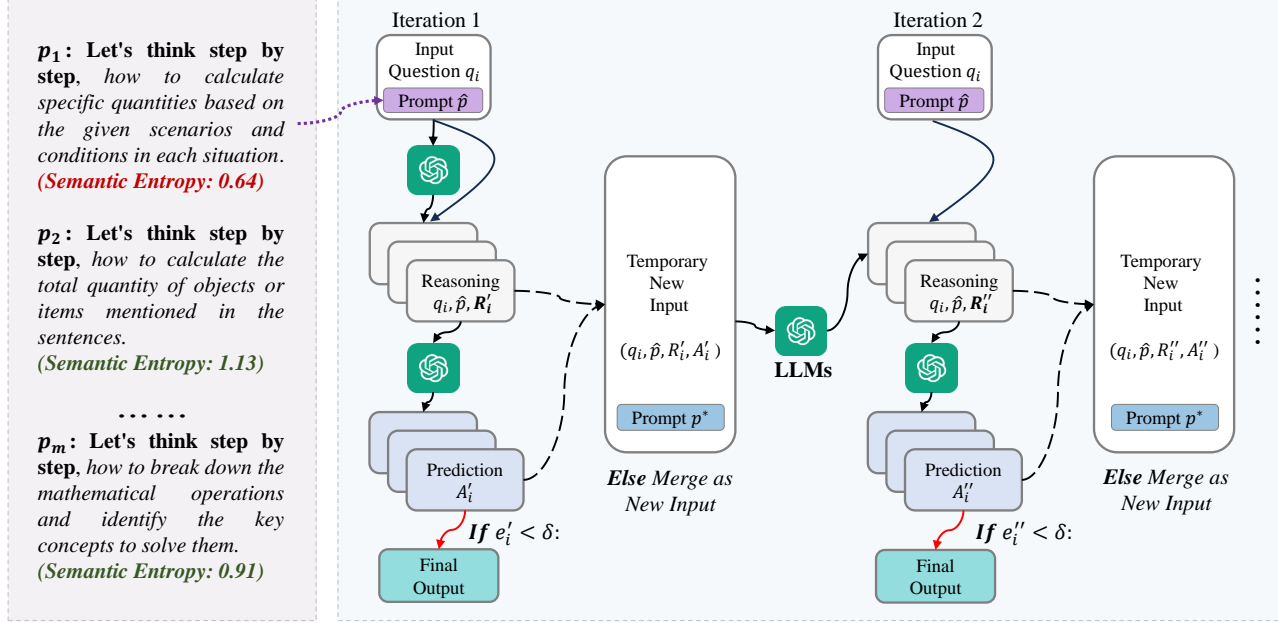


Figure 4. The flowchart of the proposed CoT framework consists of two key modules, *i.e.*, **Task-Specific Prompt** (light purple block) and **Adaptive Reasoning Iteration** (light blue block). Specifically, the task-specific prompt module first utilizes LLMs to generate m candidate prompts and evaluates their semantic entropy on the given dataset. The prompt with the lowest entropy is selected as the optimal prompt \hat{p} , providing guidance for the subsequent adaptive reasoning module to produce high-quality initial reasoning. In the adaptive reasoning iteration module, the uncertainty is calculated at each iteration and compared to a predefined threshold δ . This evaluation determines whether to accept the current prediction as the final output or to proceed to another iteration. If the uncertainty remains high, a new reasoning round is initiated with a new prompt p^* , designed to introduce diversity compared to previous reasoning steps. This iterative process continues until the uncertainty is substantially reduced or the maximum number of iterations is reached.

required for the LLMs to converge to the correct answers. Given that the initial CoT reasoning process is generated by the LLMs based on the provided prompts, this highlights the critical necessity of optimizing prompts to enhance the quality of reasoning processes from the outset.

Previous CoT methods (Wei et al., 2022; Ling et al., 2024) often rely on general prompts (*e.g.*, “Let’s think step by step”) to guide the reasoning process. Although such prompts are effective for generic tasks, they frequently fall short of capturing the nuances of domain-specific or fine-grained tasks, resulting in inadequate reasoning processes. To address this limitation, we propose a task-specific prompt module that automatically searches for the optimal prompt tailored to the task’s characteristics. Specifically, our approach begins by constructing an instruction: **# Instruction:** “Let’s think step by step” is a general prompt that can guide the LLMs to produce reasoning processes. However, in specialized domains, this prompt may lack accuracy and clarity. Below is a dataset sample. Please enhance the “Let’s think step by step, %s” prompt by adding a sentence in the %s section to better fit the dataset’s characteristics.

We then sample a question set $Q' = \{q'_1, q'_2, \dots, q'_k\}$ from the dataset \mathcal{Q} , representing the task distribution. This set Q' is concatenated with the instruction and fed into the

LLMs, which performs m rounds of sampling to generate a candidate task-specific prompt set $P = \{p_1, p_2, \dots, p_m\}$. Next, we sample another disjoint question set $Q'' = \{q''_1, q''_2, \dots, q''_k\}$ from \mathcal{Q} , ensuring $Q' \cap Q'' = \emptyset$. Each candidate prompt from P is concatenated with the questions in Q'' and used for zero-shot CoT inferences (Kojima et al., 2022). During inference, the mean semantic entropy for all questions in Q'' is calculated under each candidate prompt, yielding in the set $E = \{e_1, e_2, \dots, e_m\}$. For clarity, we define a simple mapping function $f : P \rightarrow E$ to represent the relationship between candidate prompts and their corresponding mean semantic entropy values.

Based on conclusions (i) and (iii) from the analysis of semantic entropy variation in Section 2.2, we can infer that lower semantic entropy corresponds to better CoT performance. Consequently, the prompt with the minimal semantic entropy can be regarded as the optimal prompt:

$$\hat{p} = f^{-1} (e_{\arg \min_i \{e_i | e_i \in E\}}), \quad (1)$$

where $f^{-1}(\cdot)$ function maps the minimum mean semantic entropy value back to its corresponding prompt \hat{p} . This process ensures that the selected prompt \hat{p} minimizes the semantic uncertainty associated with the specific task, thereby improving the quality of initial reasoning processes.

During the testing phase, we concatenate the optimal prompt \hat{p} derived from Eq. (1) with the question, and input the combined text into the LLMs. Following the self-consistency CoT approach (Wang et al., 2022), we perform N rounds of sampling to generate diverse reasoning processes:

$$R'_i = \{\text{LLM}(\text{Concat}(q_i, \hat{p}))_j \mid j = 1, 2, \dots, N\}, \quad (2)$$

where $\text{LLM}(\cdot)_j$ denotes the j -th sampling result produced by the LLMs, $R'_i = \{r'_{i,1}, r'_{i,2}, \dots, r'_{i,N}\}$ represents the set of reasoning processes generated, q_i corresponds to the i -th question in the dataset \mathcal{Q} , and the $\text{Concat}(\cdot)$ function refers to the sequential concatenation of the specified texts. Next, each of the N reasoning processes obtained from Eq. (2) is individually concatenated with the question q_i and the prompt \hat{p} . The resulting concatenated texts are then fed into the LLMs to generate predictions:

$$A'_i = \{\text{LLM}(\text{Concat}(q_i, \hat{p}, r'_{i,j})) \mid j = 1, \dots, N\}, \quad (3)$$

where $A'_i = \{a'_{i,1}, a'_{i,2}, \dots, a'_{i,N}\}$ represents the set of predictions generated by LLMs. At this stage, two options are available: (i) select the most frequent class from the N answers in A'_i as the final output (iteration terminates); (ii) concatenate the question q_i , the reasoning processes R'_i , and the predictions A'_i for a new round of reasoning and prediction. If option (ii) is chosen, when should the iteration be stopped? Meanwhile, how can we ensure that the newly generated reasoning and predictions surpass the previous ones? These issues will be discussed in depth in Section 3.2, where corresponding solutions will also be proposed.

3.2. Adaptive Reasoning Iteration

The conclusion (iv) presented in Section 2.2 highlights that once the reasoning processes guide the LLMs to predictions with low uncertainty, deeper iterations do not further reduce semantic entropy. Instead, such iterations often introduce noisy information, undermining predictive accuracy. This phenomenon, which we term over-reasoning, risks altering correct early predictions during subsequent iterations. To address this, we calculate the semantic entropy e'_i of the predictions A'_i and compare it against a predefined threshold δ . If $e'_i \leq \delta$, the predictions A'_i , derived from reasoning processes R'_i , is accepted as the final output. By leveraging semantic entropy to quantify the uncertainty of LLMs, we can stop iterations at the right moment to output predictions, effectively mitigating the risk of over-reasoning.

Conversely, if $e'_i > \delta$, the reasoning process proceeds to the next iteration to further reduce uncertainty. A naive solution involves concatenating the reasoning processes R'_i , predictions A'_i , and question q_i from the previous iteration while reusing the prompt \hat{p} . However, this approach often results in new reasoning processes that closely resemble previous iterations. As demonstrated by the conclusion (ii) presented

in Section 2.2, such high similarity could hinder further entropy reduction. To overcome this, we propose introducing greater divergence between reasoning iterations, enabling exploration of alternative paths and enhancing the ability of LLMs to solve complex questions. Specifically, we design a new prompt p^* to replace the \hat{p} , fostering a departure from prior reasoning steps: *# p^* : Based on the above thoughts, reevaluate from alternative perspectives to produce deeper, solution-oriented insights that go beyond prior inferences. Focus on identifying unexplored assumptions or challenges in the question context, and propose new processes.*

Then, we concatenate the new prompt p^* , the original question q_i , the previous reasoning processes R'_i , and the previous predictions A'_i to generate a new round of reasoning:

$$R''_i = \{\text{LLM}(\text{Concat}(q_i, \hat{p}, r'_{i,j}, a'_{i,j}, p^*)) \mid j = 1, \dots, N\}, \quad (4)$$

the prompt p^* encourages LLMs to critically reflect on prior information, producing reasoning steps R''_i that surpass and differ from the previous R'_i . To ensure sufficient divergence between new and previous reasoning, we measure their similarity using the Jaccard index (Jadhao & Agrawal, 2016):

$$s''_i = \text{Sim}(R''_i, R'_i) = \frac{|R''_i \cap R'_i|}{|R''_i \cup R'_i|}, s''_i \in \mathbb{R}, \quad (5)$$

if s''_i is greater than a predefined threshold τ , Eq. (4) is reapplied for resampling until the condition is met. Finally, the LLMs discard the earlier reasoning R'_i and the prediction A'_i , generating new predictions based solely on R''_i :

$$A''_i = \{\text{LLM}(\text{Concat}(q_i, \hat{p}, r''_{i,j})) \mid j = 1, \dots, N\}, \quad (6)$$

After obtaining A''_i via Eq. (6), its semantic entropy e''_i is computed and compared to δ again. If $e''_i > \delta$, the process repeats (Eqs. (4) - (6)) until the uncertainty drops to δ or the maximum iteration count T is reached.

When semantic entropy remains above δ after T iterations, three scenarios may explain this outcome: (i) previous iterations contained valid reasoning steps, but randomness in LLMs sampling introduced biases in calculating semantic entropy. Increasing N may mitigate this issue; (ii) effective reasoning paths exist but have yet to be discovered by LLMs. Extending T could allow LLMs to identify such paths; (iii) the limitations of LLMs make the question inherently unsolvable, rendering further iterations unproductive.

Although increasing T can enhance performance in the second scenario, it also escalates time and computational costs. To strike a balance between performance and efficiency, the strategy proposed in this paper is to stop further iterations when the entropy remains above δ after T iterations. Instead, we apply majority voting across the predictions from all iterations, selecting the most frequent prediction as the final output. This approach enhances overall reliability while effectively reducing computational overhead.

Method	Arithmetic					Commonsense			Symbolic		Overall
	MultiArith	GSM8K	SingleEq	AddSub	AQuA	SVAMP	STQA	CSQA	Letter	Coin	Avg. (%)
RE2	91.7	76.3	81.5	72.9	54.3	78.3	66.2	74.9	57.0	91.2	74.4
RE2 + SC	96.2	77.3	87.0	80.0	60.6	83.2	68.6	77.5	63.8	98.0	79.2
Zero-Shot	51.2	10.8	62.4	56.7	38.6	56.3	66.2	74.5	1.4	50.2	46.8
Zero-Shot-CoT	92.8	74.7	84.4	74.7	55.5	77.0	63.5	73.6	55.0	93.4	74.5
Zero-Shot-CoT + SC	95.7	79.2	88.8	81.3	63.0	82.2	65.9	75.3	66.2	97.2	79.5
+ TSP	97.0	81.1	90.0	84.8	65.7	85.5	66.7	76.7	68.4	97.6	81.4
	(+1.3)	(+1.8)	(+1.2)	(+3.5)	(+2.7)	(+3.3)	(+0.8)	(+1.3)	(+2.2)	(+0.4)	(+1.9)
+ ARI	96.7	82.6	92.1	87.1	69.3	87.1	67.5	77.5	75.8	97.2	83.3
	(+1.0)	(+3.4)	(+3.3)	(+5.8)	(+6.3)	(+4.9)	(+1.6)	(+2.2)	(+9.6)	(+0.0)	(+3.8)
+ TSP + ARI	98.2	83.0	92.9	88.4	70.1	87.5	66.7	76.7	77.2	96.4	83.7
	(+2.5)	(+3.8)	(+4.1)	(+7.1)	(+7.1)	(+5.3)	(+0.8)	(+1.4)	(+11.0)	(-0.8)	(+4.2)

Table 1. Accuracy (%) across ten reasoning datasets from three categories of zero-shot reasoning tasks. The number of self-consistency (SC) sampling is fixed at 3 for all cases. Blue and red fonts indicate increases and decreases in task performance compared to the “Zero-Shot-CoT + SC” method, respectively, while bold font highlights the best performance in each column.

4. Experiments

4.1. Experimental Settings

We evaluate our CoT framework on 10 reasoning datasets, including six arithmetic datasets (*i.e.*, MultiArith (Roy & Roth, 2016), GSM8K (Cobbe et al., 2021), SingleEq (Koncel-Kedziorski et al., 2015), AddSub (Hosseini et al., 2014), AQuA (Ling et al., 2017), and SVAMP (Patel et al., 2021)), two commonsense reasoning datasets (*i.e.*, StrategyQA (Geva et al., 2021) and CommonsenseQA (Talmor et al., 2018)), and two symbolic reasoning datasets (*i.e.*, LastLetter and CoinFlip (Wei et al., 2022)). We utilize GPT-3.5-turbo-0125 as the foundation model for all experiments, given its accessibility and cost-effectiveness.

Our evaluation adopts a progressive comparative approach. Specifically, we first test zero-shot reasoning by directly inputting questions into the LLMs without prompts. Next, we employ zero-shot CoT (Kojima et al., 2022), utilizing general prompts with greedy decoding to generate answers. Finally, we implement zero-shot CoT with self-consistency (Wang et al., 2022), which enhances accuracy through multiple decoding attempts and a voting mechanism. Building on these baselines, we propose a novel CoT framework comprising two modules, *i.e.*, task-specific prompt (TSP) and adaptive reasoning iteration (ARI). The TSP module improves the initial CoT reasoning process by replacing generic prompts with task-specific ones, while the ARI module further enhances task performance through iterative refinement of the reasoning process. Moreover, we also compared two popular CoT methods, *i.e.*, RE2 (Xu et al., 2024) and Contrastive-CoT (Chia et al., 2023).

4.2. Main Results

We followed literature (Kojima et al., 2022) to construct zero-shot reasoning tasks across all 10 datasets, and performed few-shot reasoning tasks on the MultiArith and

Method	MultiArith	GSM8K	Avg. (%)
Contrastive-CoT	89.7	69.4	79.6
Contrastive-CoT + SC	93.0	71.9	82.5
Few-Shot	78.3	53.8	66.1
Few-Shot-CoT	94.3	69.1	81.7
Few-Shot-CoT + SC	97.2	73.7	85.5
+ ARI	97.3	77.4	87.4
	(+0.1)	(+3.7)	(+1.9)

Table 2. Accuracy across the MultiArith and GSM8K datasets from the arithmetic category of few-shot reasoning tasks. The number of self-consistency (SC) samplings is fixed at 3 for all cases.

GSM8K datasets. The results of these experiments are presented in Table 1 and Table 2, respectively.

For the zero-shot task, the baseline zero-shot method achieves an overall average accuracy of 46.8%. Incorporating CoT reasoning (Zero-Shot-CoT) significantly enhances performance, raising the accuracy to 74.5%. Further improvement is observed with the integration of self-consistency (SC), which increases the average accuracy to 79.5%. Building on this foundation, the addition of task-specific prompt (TSP) and adaptive reasoning iteration (ARI) modules further elevates the average accuracy to 83.7%. This represents a 4.2% improvement over the SC approach, demonstrating the advantages of our method across various task categories. Furthermore, our method showed the most significant performance on arithmetic datasets. Specifically, compared to the SC approach, the average performance across six datasets increased from 81.7% to 86.7%. This improvement can be attributed to the fact that deep reasoning enables the LLMs to systematically identify solution pathways. In contrast, the performance gains on commonsense datasets are relatively weak, even approaching the level of the zero-shot method. This limitation may arise from the dependency of these tasks on the prior knowledge of the LLMs. If the relevant commonsense knowledge was not encountered during pre-training, deep reasoning alone is insufficient to address the question.

In the few-shot task, the SC approach achieves an average accuracy of 85.4%. The incorporation of the ARI module results in a significant performance improvement, raising the accuracy to 87.4%. However, the TSP module is not applicable to few-shot tasks, as the LLMs have already utilized the limited examples provided to generate optimal reasoning in the initial iteration, rendering the reconstruction of a new reasoning process through TSP unnecessary.

Based on the above analysis, it is evident that the proposed ARI module enhances performance in both zero-shot and few-shot tasks, demonstrating its potential as a plug-and-play solution applicable across all CoT methods. Similarly, the TSP module can be applied to zero-shot methods to improve the quality of reasoning in the initial iteration. Ablation experiments presented in the last four rows of Table 2 confirm that, compared to the ARI module alone, the TSP module contributes an average performance improvement of 0.4%, thereby validating its effectiveness.

4.3. Adaptive Versus Fixed Iterative Reasoning

To further verify the effectiveness of our proposed method, we compared its accuracy and time costs with the fixed iterative reasoning approach on the AQuA dataset.

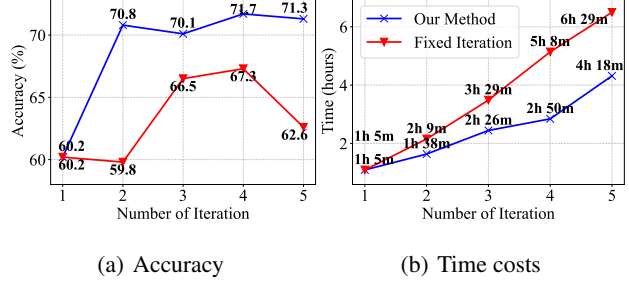
4.3.1. COMPARISON OF ACCURACY AND TIME COSTS

In terms of accuracy (see Figure 5(a)), our method demonstrates a clear advantage. It achieves 70.8% at the second iteration and maintains stability, reaching 71.3% by the fifth iteration. In contrast, the fixed iteration method shows slower improvement, peaking at 67.3% and then dropping to 62.6% by the fifth iteration. Regarding time cost (see Figure 5(b)), both methods exhibit a linear growth trend, but our method is significantly more time-efficient. The time cost of our approach increases gradually from 1 hour and 5 minutes at the first iteration to 4 hours and 18 minutes at the fifth iteration, reflecting a moderate growth rate. In comparison, the fixed iteration method follows a steeper trajectory, with the time cost rising from 1 hour and 5 minutes to 6 hours and 29 minutes by the fifth iteration.

Overall, our adaptive iteration outperforms fixed iteration in both effectiveness and efficiency, achieving an optimal balance between the two as early as the second iteration, highlighting its practicality and strong performance.

4.3.2. WHY OUR METHOD WORKS?

Our proposed method significantly surpasses fixed reasoning iteration by effectively addressing two critical challenges: (i) over-reasoning, and (ii) high similarity between consecutive reasoning iterations. To resolve the issue of over-reasoning, we incorporate a mechanism that quantifies the prediction uncertainty of the LLMs using semantic



(a) Accuracy

(b) Time costs

Figure 5. Accuracy and time costs of adaptive reasoning iteration compared to the fixed reasoning iteration on the AQuA dataset.

entropy. The iteration process is terminated as soon as a low-uncertainty state is reached, ensuring predictions are made at the optimal stage. For example, as illustrated in Table 6, the semantic entropy after the first iteration falls below the predefined threshold of 0.95 (indicating that at least two out of three elements in the prediction set are consistent). At this point, further iterations are deemed unnecessary, and the current prediction is finalized as the output.

When the uncertainty is high and further iterations are required, the issue of high similarity between consecutive iterations may arise. To address this, we propose a novel prompt p^* to encourage greater divergence in subsequent reasoning iterations, with the Jaccard index introduced to quantify this diversity. If insufficient diversity is detected, the reasoning process is resampled until predefined conditions are met. This strategy effectively ensures the diversity and independence of consecutive reasoning iterations. For example, as detailed in Table 6, the prompt p^* and resampling strategy successfully guided the LLMs to generate more distinct reasoning paths, transforming an initial incorrect prediction into a correct one. Furthermore, as shown in Table 4, our method achieves lower similarity between consecutive iterations compared to existing approaches.

By dynamically adjusting reasoning iterations and promoting diversity in reasoning paths, our approach enhances accuracy while significantly reducing computational costs.

5. Conclusion

This paper explores the conceptual parallels between chain-of-thought (CoT) reasoning and self-training, identifying their shared objective of iteratively leveraging information augmentation to minimize prediction uncertainty. Through theoretical analysis and experimental validation, we reveal semantic entropy dynamics in CoT reasoning and propose improvements, including a task-specific prompt module to optimize initial reasoning processes and an adaptive reasoning iteration module to mitigate over-reasoning and enhance reasoning diversity in consecutive iterations. Collectively, these innovations significantly improve the performance of CoT reasoning in addressing complex tasks.

References

Amini, M.-R., Feofanov, V., Paletto, L., Hadjadj, L., Devijver, E., and Maximov, Y. Self-training: A survey. *Neurocomputing*, pp. 128904, 2024.

Bartlett, P., Freund, Y., Lee, W. S., and Schapire, R. E. Boosting the margin: A new explanation for the effectiveness of voting methods. *The annals of statistics*, 26(5):1651–1686, 1998.

Chen, B., Jiang, J., Wang, X., Wan, P., Wang, J., and Long, M. Debiased self-training for semi-supervised learning. In *NeurIPS*, volume 35, pp. 32424–32437, 2022.

Chia, Y. K., Chen, G., Tuan, L. A., Poria, S., and Bing, L. Contrastive chain-of-thought prompting. *arXiv preprint arXiv:2311.09277*, 2023.

Chu, Z., Chen, J., Chen, Q., Yu, W., He, T., Wang, H., Peng, W., Liu, M., Qin, B., and Liu, T. Navigate through enigmatic labyrinth a survey of chain of thought reasoning: Advances, frontiers and future. In *ACL*, pp. 1173–1203, 2024.

Cobbe, K., Kosaraju, V., Bavarian, M., Chen, M., Jun, H., Kaiser, L., Plappert, M., Tworek, J., Hilton, J., Nakano, R., et al. Training verifiers to solve math word problems. *arXiv preprint arXiv:2110.14168*, 2021.

Farquhar, S., Kossen, J., Kuhn, L., and Gal, Y. Detecting hallucinations in large language models using semantic entropy. *Nature*, 630(8017):625–630, 2024.

Frei, S., Zou, D., Chen, Z., and Gu, Q. Self-training converts weak learners to strong learners in mixture models. In *AISTATS*, pp. 8003–8021, 2022.

Geva, M., Khashabi, D., Segal, E., Khot, T., Roth, D., and Berant, J. Did aristotle use a laptop? a question answering benchmark with implicit reasoning strategies. *Transactions of the Association for Computational Linguistics*, 9:346–361, 2021.

Grandvalet, Y. and Bengio, Y. Semi-supervised learning by entropy minimization. In *NeurIPS*, volume 17, 2004.

Hosseini, M. J., Hajishirzi, H., Etzioni, O., and Kushman, N. Learning to solve arithmetic word problems with verb categorization. In *EMNLP*, pp. 523–533, 2014.

Jadhai, A. and Agrawal, A. Text categorization using jaccard coefficient for text messages. *International Journal of Science and Research*, 5(5):2047–2050, 2016.

Kojima, T., Gu, S. S., Reid, M., Matsuo, Y., and Iwasawa, Y. Large language models are zero-shot reasoners, 2022.

Koncel-Kedziorski, R., Hajishirzi, H., Sabharwal, A., Etzioni, O., and Ang, S. D. Parsing algebraic word problems into equations. *Transactions of the Association for Computational Linguistics*, 3:585–597, 2015.

Lanham, T., Chen, A., Radhakrishnan, A., Steiner, B., Denison, C., Hernandez, D., Li, D., Durmus, E., Hubinger, E., Kernion, J., et al. Measuring faithfulness in chain-of-thought reasoning. *arXiv preprint arXiv:2307.13702*, 2023.

Lee, D.-H. et al. Pseudo-label: The simple and efficient semi-supervised learning method for deep neural networks. In *ICML*, pp. 896, 2013.

Lin, Z., Chan, C., Song, Y., and Liu, X. Constrained reasoning chains for enhancing theory-of-mind in large language models. *arXiv preprint arXiv:2409.13490*, 2024.

Ling, W., Yogatama, D., Dyer, C., and Blunsom, P. Program induction by rationale generation: Learning to solve and explain algebraic word problems. In *ACL*, pp. 158–167, 2017.

Ling, Z., Fang, Y., Li, X., Huang, Z., Lee, M., Memisevic, R., and Su, H. Deductive verification of chain-of-thought reasoning. In *NeurIPS*, volume 36, 2024.

Miyato, T., Maeda, S.-i., Koyama, M., and Ishii, S. Virtual adversarial training: a regularization method for supervised and semi-supervised learning. *IEEE transactions on pattern analysis and machine intelligence*, 41(8):1979–1993, 2018.

Mukherjee, S. and Awadallah, A. Uncertainty-aware self-training for few-shot text classification. In *NeurIPS*, volume 33, pp. 21199–21212, 2020.

Nayab, S., Rossolini, G., Buttazzo, G., Manes, N., and Giacomelli, F. Concise thoughts: Impact of output length on llm reasoning and cost. *arXiv preprint arXiv:2407.19825*, 2024.

Patel, A., Bhattacharya, S., and Goyal, N. Are nlp models really able to solve simple math word problems? *arXiv preprint arXiv:2103.07191*, 2021.

Roy, S. and Roth, D. Solving general arithmetic word problems. *arXiv preprint arXiv:1608.01413*, 2016.

Scudder, H. Adaptive communication receivers. *IEEE Transactions on Information Theory*, 11(2):167–174, 1965.

Sun, J., Zheng, C., Xie, E., Liu, Z., Chu, R., Qiu, J., Xu, J., Ding, M., Li, H., Geng, M., et al. A survey of reasoning with foundation models. *arXiv preprint arXiv:2312.11562*, 2023.

Talmor, A., Herzig, J., Lourie, N., and Berant, J. Commonsenseqa: A question answering challenge targeting commonsense knowledge. *arXiv preprint arXiv:1811.00937*, 2018.

Tur, G., Hakkani-Tür, D., and Schapire, R. E. Combining active and semi-supervised learning for spoken language understanding. *Speech Communication*, 45(2):171–186, 2005.

Wang, L., Xu, W., Lan, Y., Hu, Z., Lan, Y., Lee, R. K.-W., and Lim, E.-P. Plan-and-solve prompting: Improving zero-shot chain-of-thought reasoning by large language models. *arXiv preprint arXiv:2305.04091*, 2023.

Wang, X., Wei, J., Schuurmans, D., Le, Q., Chi, E., Narang, S., Chowdhery, A., and Zhou, D. Self-consistency improves chain of thought reasoning in language models. *arXiv preprint arXiv:2203.11171*, 2022.

Wei, J., Wang, X., Schuurmans, D., Bosma, M., Xia, F., Chi, E., Le, Q. V., Zhou, D., et al. Chain-of-thought prompting elicits reasoning in large language models. In *NeurIPS*, volume 35, pp. 24824–24837, 2022.

Xu, X., Tao, C., Shen, T., Xu, C., Xu, H., Long, G., Lou, J.-G., and Ma, S. Re-reading improves reasoning in large language models. In *EMNLP*, pp. 15549–15575, 2024.

Yang, X., Song, Z., King, I., and Xu, Z. A survey on deep semi-supervised learning. *IEEE Transactions on Knowledge and Data Engineering*, 35(9):8934–8954, 2022.

Zhang, B., Wang, Y., Hou, W., Wu, H., Wang, J., Okumura, M., and Shinohzaki, T. Flexmatch: Boosting semi-supervised learning with curriculum pseudo labeling. *Advances in Neural Information Processing Systems*, 34: 18408–18419, 2021.

Zhang, Z., Zhang, A., Li, M., and Smola, A. Automatic chain of thought prompting in large language models. *arXiv preprint arXiv:2210.03493*, 2022.

Zhong, T., Liu, Z., Pan, Y., Zhang, Y., Zhou, Y., Liang, S., Wu, Z., Lyu, Y., Shu, P., Yu, X., et al. Evaluation of openai o1: Opportunities and challenges of agi. *arXiv preprint arXiv:2409.18486*, 2024.

Zou, Y., Yu, Z., Kumar, B., and Wang, J. Unsupervised domain adaptation for semantic segmentation via class-balanced self-training. In *Proceedings of the European conference on computer vision (ECCV)*, pp. 289–305, 2018.

Zou, Y., Yu, Z., Liu, X., Kumar, B., and Wang, J. Confidence regularized self-training. In *CVPR*, pp. 5982–5991, 2019.

A. Appendix

A.1. Omitted Definitions and Proofs in Section 2.1

In this section, we supplement the definitions and detailed algorithm of self-training that were not elaborated in Section 2.1 and provide the proofs of Lemma 2.1 and Theorem 2.2. Our results primarily reference (Frei et al., 2022), and most definitions and algorithms will adopt the settings from their work. Here, we consider a very simple mixture Gaussian model (GMM) rather than adopting the more general but relatively more complex sub-exponential distribution with parameters K, U, U', R as defined in (Frei et al., 2022).

Definition A.1 (Gaussian Mixture Model). A joint distribution $(x, y) \sim \mathcal{D}$ over $\mathbb{R}^d \times \{\pm 1\}$ is called Gaussian mixture model, if $y \sim \text{Unif}(\{\pm 1\})$, and $x|y \sim \mathcal{N}(y\mu, I)$, where $\mu \in \mathbb{R}^d$ is the mean of \mathcal{D} . We use \mathcal{D}_x to denote the marginal distribution of \mathcal{D} .

The information entropy of a discrete random variable X is defined as $\text{Ent}[X] = \mathbb{E}[-\log X] = -\sum_{x \in \mathcal{X}} p(x) \log p(x)$, where \mathcal{X} is the set of values that the random variable X can take. A classifier for the Gaussian mixture model is given by $x \mapsto \text{sgn}(\beta^T x)$, where $\beta \in \mathbb{R}^d$ is an arbitrary vector. So we use β to denote a classifier without saying $x \mapsto \text{sgn}(\beta^T x)$. According to Fact 3.4 in (Frei et al., 2022), the Bayes-optimal classifier of the Gaussian mixture model defined in Definition A.1 is μ . Assume we can access a initial classifier pseudo-labeler β_{init} , which is also called a pseudo-labeler, and the population error of β_{init} is sufficiently small but constant. We then use a weight-normalized logistic regression method to train start from β_{init} using only unlabeled samples. The loss function is $\ell(z) = \log(1 + \exp(-z))$. Let $\sigma > 0$ be temperature. The training dataset S is partitioned into T batches of size B . The general process of the self-training algorithm involves multiple iterations, where in each iteration, a batch of data is assigned pseudo-labels. The data labeled in this iteration, along with the existing labeled data and data pseudo-labeled in previous iterations, is used to update the model. This process continues until all samples have been assigned pseudo-labels. The detailed and formal algorithm description of self training using the pseudo-label strategy is presented in Algorithm 1.

Algorithm 1 Self-Training

```

1: input: Training dataset  $S = \{x_i^{(t)}\}_{\substack{1 \leq i \leq B \\ 0 \leq t \leq T-1}}$ , step size  $\eta$ , temperature  $\sigma > 0$ , initial pseudo-labeler  $\beta_{\text{init}}$ 
2:  $\beta_0 \leftarrow \beta_{\text{init}} / \|\beta_{\text{init}}\|$ ; {model initialization}
3: for  $t = 0, \dots, T-1$  do
4:   Generate pseudo-labels  $\hat{y}_i^{(t)} = \text{sgn}(\beta_t^T x_i^{(t)})$  for batch  $\{x_i^{(t)}\}_{1 \leq i \leq B}$ ; {information augmentation}
5:    $\tilde{\beta}_{t+1} = \beta_t - \frac{\eta}{B} \sum_{i=1}^B \nabla \ell\left(\frac{1}{\sigma} \cdot \hat{y}_i^{(t)} \cdot (\beta_t^T x_i^{(t)})\right)$ ;
6:    $\beta_{t+1} = \tilde{\beta}_{t+1} / \|\tilde{\beta}_{t+1}\|$ ; {update model}
7: end for
8: output:  $\beta_{T-1}$ ;

```

A.1.1. PROOF OF LEMMA 2.1

We first restate Lemma 2.1.

Lemma A.2 (Lemma 2.1, restate). *Suppose $(x, y) \sim \mathcal{D}$ follows a mixture Gaussian models in $\mathbb{R}^d \times \{\pm 1\}$ with mean μ satisfying $\|\mu\| = \Theta(1)$, i.e., $y \sim \text{Unif}(\{\pm 1\})$ and $x|y \sim \mathcal{N}(y\mu, I)$. Let $\ell(z) = \log(1 + \exp(-z))$, and assume $\sigma \geq \max(1, \|\mu\|)$. Assume we can access a initial pseudo-labeler β_{init} which satisfies $\Pr_{(x,y) \sim \mathcal{D}}[y \neq \text{sgn}(\beta_{\text{init}}^T x)] = O(1)$. Let $\varepsilon, \delta \in (0, 1)$, and assume that $B = \tilde{\Omega}(\varepsilon^{-1})$, $T = \tilde{\Omega}(\varepsilon^{-1})$, $\eta = \tilde{\Theta}(d^{-1}\varepsilon)$, suppose θ_t is the angle between β_t and μ , then by running algorithm 1 with step size η and batch size B , when $t < T-1$, $\theta_t \geq \theta_{t+1}$ holds with probability at least $1 - \delta$, and with probability at least $1 - \delta$, $\theta_{T-1} \leq O(\varepsilon)$.*

Proof. To prove this lemma, We first present the results on sample complexity for labeled and unlabeled data obtained in (Frei et al., 2022) for self-training. Theorem 4.1 in (Frei et al., 2022) ensures that we can obtain a classifier with sufficiently small but constant error. More precisely, a standard logistic regression procedure produces a pseudolabler that can achieve the desired constant accuracy by using $O(d)$ labeled samples, which essentially represents the sample complexity of labeled data. As for the unlabeled data, the sample complexity is expressed in the lemma below.

Lemma A.3 (The Sample Complexity for Unlabeled Data, Theorem 3.6 in (Frei et al., 2022)). *Suppose that $(x, y) \sim \mathcal{D}$ follows a mixture distribution with mean μ satisfying $\|\mu\| = \Theta(1)$ and parameters $K, U, U', R = \Theta(1)$. Let ℓ be well-behaved for some $C_\ell \geq 1$, and assume the temperature satisfies $\sigma \geq \max(R, \|\mu\|)$. Assume access to a pseudo-labeler β_{init} which satisfies $\Pr_{(x,y) \sim \mathcal{D}}(y \neq \text{sgn}(\beta_{\text{init}}^T x)) \leq C_{\text{err}}$, where $C_{\text{err}} = R^2/(72C_\ell U')$. Let $\varepsilon, \delta \in (0, 1)$, and assume that $B = \tilde{\Omega}(\varepsilon^{-1})$, $T = \tilde{\Omega}(d\varepsilon^{-1})$, $\eta = \tilde{\Theta}(d^{-1}\varepsilon)$. Then with probability at least $1 - \delta$, by running Algorithm 1 with step size η and batch size B , the last iterate satisfies $\text{err}(\beta_{T-1}) \leq \text{err}(\mu) + \varepsilon$. In particular, $T = \tilde{O}(d/\varepsilon)$ iterations using at most $TB = \tilde{O}(d/\varepsilon^2)$ unlabeled samples suffices to be within ε error of the Bayes-optimal classifier.*

Some definitions mentioned in Lemma A.3 can be found in the original paper and are omitted here due to space constraints. We use the function $\ell(z) = \log(1 + \exp(-z))$ as our loss function and it's well behaved. For GMM, it is a mixture distribution with parameters $K, U, U', R = \Theta(1)$. Under the conditions of Lemma A.3, let $\bar{\mu} = \mu / \|\mu\|$. We can derive the following lemma regarding $\|\beta_t - \bar{\mu}\|$, which represents the distance between the classifier produced at each iteration of the algorithm and the normalized optimal classifier.

Lemma A.4 (Recursion of Δ_t^2 , Lemma D.2 in (Frei et al., 2022)). *Suppose $\Delta_t^2 = \|\beta_t - \bar{\mu}\|^2$, then Δ_t^2 satisfies that for $1 \leq t \leq T$,*

$$\Delta_t^2 \leq (1 - \eta/2C_g)\Delta_{t-1}^2 + \frac{\eta\varepsilon}{8C_g} + \frac{2C_d\eta^2}{\sigma^2},$$

where C_g, C_d, σ are all some positive constants such that $K = C_d C_g^2 \sigma^2 \geq 1$, $\Delta_0 \leq 2$.

Note that there is close relationship between θ_t and Δ_t , we can use the changes in Δ_t described in Lemma A.4 to characterize the changes in θ_t , leading to the following lemma.

Lemma A.5. *Let θ_t denote the angle between β_t and μ , $\theta_t \in (0, \pi/2)$, and $\Delta_t^2 = \|\beta_t - \bar{\mu}\|^2$. Then for $1 \leq t < T-1$, $\theta_t \geq \theta_{t+1}$, and $\theta_T \leq \varepsilon$.*

Proof. Since β_t and $\bar{\mu}$ both have unit norm, it's easy to verify that

$$\|\beta_t - \bar{\mu}\|^2 = 2(1 - \cos \theta) = 4 \sin^2 \frac{\theta_t}{2}$$

It's sufficient to assume that $\theta_t \in (0, \pi/2)$ for any t , as the error rate of β_{init} is sufficiently small. Therefore $\Delta_t = 2 \sin \frac{\theta_t}{2}$, i.e., $\theta_t = 2 \arcsin \frac{\Delta_t}{2}$. This implies that θ_t and Δ_t share the same monotonicity, so it suffices to show that for $t < T$, $\Delta_t \leq \Delta_{t-1}$. By Lemma A.4, when $\eta = \frac{\varepsilon C_g}{16K}$ and $T \geq 32K\varepsilon^{-1} \log(32K\varepsilon^{-1})$, it's easy to verify that $\Delta_T \leq \varepsilon$, which means that $\Delta_t > \varepsilon$ for $t < T$. Hence, with the recursion of Δ_t^2 in Lemma A.4, we have

$$\begin{aligned} \Delta_t^2 - \Delta_{t-1}^2 &\leq -\frac{\eta}{2C_g}\Delta_{t-1} + \frac{\eta\varepsilon}{8C_g} + \frac{2C_d\eta^2}{\sigma^2} \\ &= -\frac{\eta}{2C_g} \left(\Delta_{t-1} - \left(\frac{1}{4} + \frac{1}{4\sigma^4} \right) \varepsilon \right) \\ &\leq -\frac{\eta}{2C_g} (\Delta_{t-1} - \varepsilon) \\ &\leq 0 \end{aligned}$$

At the same time, $\theta_T = 2 \arcsin \frac{\Delta_T}{2} = \Theta(\Delta_T) = O(\varepsilon)$. This concludes the proof. \square

Finally, through the conditions and assumptions of Lemma A.3, along with the conclusion of Lemma A.5, we complete the proof of Lemma 2.1. \square

A.1.2. PROOF OF THEOREM 2.2

Theorem A.6 (Theorem 2.2, restate). *Under the assumptions of Lemma 2.1, let $d = 2$ and suppose $\hat{y}^{(t)}|x \sim \text{Ber}(\vartheta(\beta_t^T x))$ is the pseudo-label of x , where $\vartheta(z) = \frac{1}{1+\exp(-z)}$. Define $l(\alpha)$ as the line $x^T \alpha^\perp = 0$, where α^\perp is perpendicular to α . Let $A(\alpha_1, \alpha_2)$ denote the region swept by $l(\alpha_1)$ rotating to $l(\alpha_2)$ along the trajectory of β_{init} towards μ during self-training. Denote $H_t(x) = \text{Ent}[\hat{y}^{(t)}|x]$ be the entropy of $\hat{y}^{(t)}|x$. For $t < T$, with probability at least $1 - \delta$, the entropy changes as follows: (i) $H_t(x)$ first decreases and then increases if $x \in A(\beta_0, \mu)$; (ii) $H_t(x)$ decreases if $x \in A(\mu, \beta_0^\perp)$; (iii) $H_t(x)$ first increases and then decreases if $x \in A(\beta_0^\perp, \mu^\perp)$; and (iv) $H_t(x)$ increases if $x \in A(\mu^\perp, \beta_0)$.*

Proof. Lemma 2.1 describes the trend in the changes of the vector corresponding to the classifier, which is particularly useful for analyzing entropy changes in \mathbb{R}^2 , as the entropy of the pseudo-label distribution is directly related to the angle between the classifier and the samples. Since we define the pseudo-label distribution as a Bernoulli distribution using the sigmoid function, we first present the following lemma on the entropy of a Bernoulli distribution.

Lemma A.7. *Let $X \sim \text{Ber}(p)$, $p \in [0, 1]$. Then $\text{Ent}[X]$ is a decreasing function of $|p - 1/2|$, i.e., if $X_1 \sim \text{Ber}(p_1)$, $X_2 \sim \text{Ber}(p_2)$, then $\text{Ent}[X_1] \geq \text{Ent}[X_2]$ if and only if $|p_1 - 1/2| \leq |p_2 - 1/2|$.*

Proof. For $X \sim \text{Ber}(p)$, $\text{Ent}[X] = f(p) = -p \log p - (1-p) \log(1-p)$. We define $0 \log 0 = 0$. It is easy to verify that $f(p)$ is symmetric about the line $x = 1/2$. On $(0, 1/2)$, $f(p)$ is monotonically increasing, and on $(1/2, 1)$, $f(p)$ is monotonically decreasing. Thus, for X_1 and X_2 , $\max(p_1, 1-p_1) \in (1/2, 1)$ and $\max(p_2, 1-p_2) \in (1/2, 1)$, by the monotonicity and symmetry of $f(p)$, it is straightforward to conclude that $\text{Ent}(X_1) \geq \text{Ent}(X_2)$ if and only if $\max(p_1, 1-p_1) \leq \max(p_2, 1-p_2)$. Moreover, $\max(p_1, 1-p_1) \leq \max(p_2, 1-p_2)$ if and only if $|p_1 - 1/2| \leq |p_2 - 1/2|$, which completes the proof. \square

Now, we analyze the monotonic properties of $H_t(x)$. From Lemma A.7, we know that for $X \sim \text{Ber}(p)$, $\text{Ent}[X]$ depends on the magnitude of $|p - 1/2|$. In the subsequent proof, we establish the conclusion that during the iteration process, if $\vartheta(\beta_t^T x) < 1/2$, it will not happen that $\vartheta(\beta_{t+1}^T x) > 1/2$ unless $\vartheta(\beta_t^T x)$ is very close to $1/2$, causing $\vartheta(\beta_{t+1}^T x) > 1/2$ in the next iteration. This essentially states that in the self-training process, pseudo-labels do not fluctuate across iterations. Therefore, we only need to consider the relationship between $\vartheta(\beta_t^T x)$ and $\vartheta(\beta_{t+1}^T x)$.

Since $\vartheta(z) = \frac{1}{1+\exp(-z)}$ is monotonically increasing, it suffices to compare $\beta_t^T x$ and $\beta_{t+1}^T x$. Let the angle between β_t and x be $\theta^{(t)}(x) \in (0, \pi)$. Then, $\beta_t^T x = \|x\| \cos \theta^{(t)}(x) = \text{sgn}(\|x\| \cos \theta^{(t)}(x)) \|x\| |\cos \theta^{(t)}(x)|$. For the same sample, we only need to consider the changes in $\theta^{(t)}(x)$ as t varies and the monotonicity of the function $f(z) = |\cos(z)|$ on $(0, \pi)$ ($f(z)$ is decreasing on $z \in (0, \pi/2)$ and increasing on $z \in (\pi/2, \pi)$). Define the angle between x and μ as $\theta^{(\infty)}(x)$.

We now discuss the four regions defined in the theorem respectively.

1. $x \in A(\beta_0, \mu)$. When $\theta^{(0)}(x) \in (0, \pi/2)$ and $\theta^{(0)}(x) \leq \theta_0$, x can be considered to lie between vector β_0 and vector μ . If $\theta_t \geq \theta^{(t)}(x)$, then $\theta^{(t)}(x) = \theta_t - (\theta_0 - \theta^{(0)}(x)) \in (0, \pi/2)$; if $\theta_t \leq \theta^{(t)}(x)$, then $\theta^{(t)}(x) = (\theta_0 - \theta^{(0)}(x)) - \theta_t \in (0, \pi/2)$. Therefore, $\theta^{(t)}(x)$ first increases and then decreases, remaining within the interval $(0, \pi/2)$, which implies that $H_t(x)$ first decreases and then increases. The proof for the other case is similar.
2. $x \in A(\mu, \beta_0^\perp)$. When $\theta^{(0)}(x) \in (0, \pi/2)$ and $\theta^{(0)}(x) > \theta_0$, x can be considered to lie between vector μ and β_0^\perp , with the angle between β_0^\perp and μ lying in $(0, \pi/2)$. In this case, $\theta^{(t)}(x) = \theta_t + \theta^{(\infty)}(x) \in (0, \pi/2)$, so $\theta^{(t)}(x)$ decreases monotonically and remains in $(0, \pi/2)$, implying that $H_t(x)$ decreases monotonically. The other case is similar.
3. $x \in A(\beta_0^\perp, \mu^\perp)$. When $\theta^{(0)}(x) \in (\pi/2, \pi)$ and $\theta^{(\infty)}(x) \in (0, \pi/2)$, x can be considered to lie between vector β_0^\perp and μ^\perp , where the angle between β_0^\perp and μ , as well as the angle between μ^\perp and β_0^\perp , both lie in $(0, \pi/2)$. In this case, $\theta^{(t)}(x) = \theta_t + \theta^{(\infty)}(x)$ decreases monotonically, but there exists some t' such that β_t becomes orthogonal to x , leading to $H_t(x)$ first increasing and then decreasing. The proof for the other case is similar.
4. $x \in A(\mu^\perp, \beta_0)$. When $\theta^{(0)}(x) \in (\pi/2, \pi)$ and $\theta^{(\infty)}(x) \in (\pi/2, \pi)$, x can be considered to lie between μ^\perp and $-\beta_0$. In this case, $\theta^{(t)}(x) = \theta_t + \theta^{(\infty)}(x) \in (\pi/2, \pi)$ decreases monotonically, implying that $H_t(x)$ increases monotonically. The proof for the other case is similar.

Through the above analysis, we complete the proof of Theorem 2.2. \square

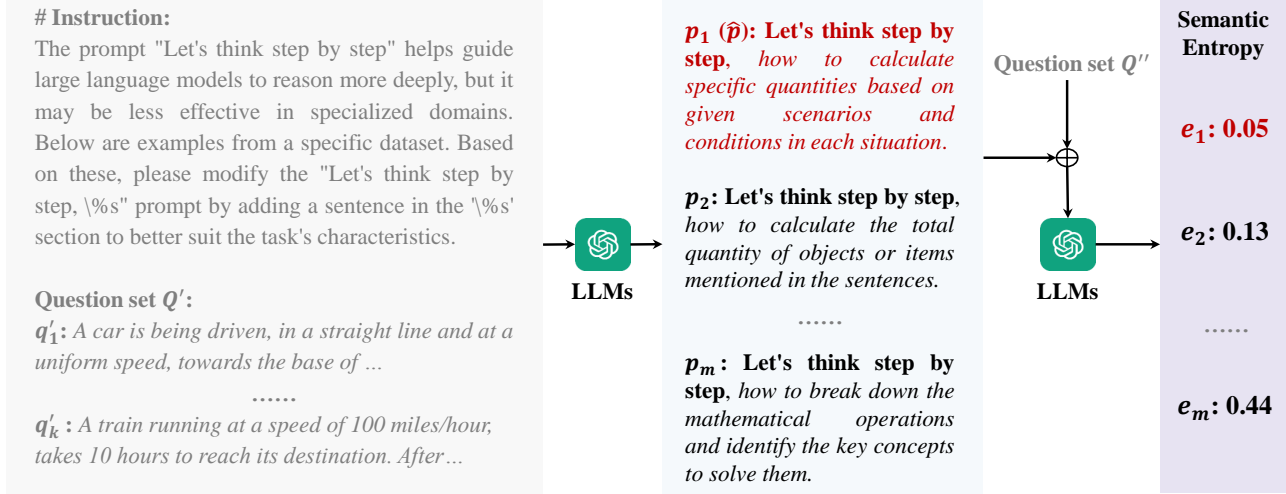


Figure 6. The proposed **Task-Specific Prompt** module tailors the prompt to the characteristics of a given task. Initially, a set of candidate prompts $\{p_1, p_2, \dots, p_m\}$ is generated by incorporating a tailored instruction and a question set, Q' sampled from the dataset. Next, another disjoint question set Q'' is sampled, distinct from Q' . The candidate prompts $\{p_1, p_2, \dots, p_m\}$ are then evaluated based on their semantic entropy values $\{e_1, e_2, \dots, e_m\}$, and the prompt \hat{p} with the lowest entropy is selected as the optimal one for the task.

A.2. Related Work

A.2.1. SELF-TRAINING

Self-training (Scudder, 1965) has become a popular semi-supervised learning approach in recent years, which focuses on utilizing pseudo-labeling strategies to enlarge labeled datasets (Yang et al., 2022). A well-crafted pseudo-labeling strategy ensures that pseudo-labels for unlabeled data match the distribution of labeled datasets. Current research primarily concentrates on the selection of high-confidence pseudo-labels, and the training of multi-classifier models (Amini et al., 2024). In the selection of pseudo-labels, some works directly choose unlabeled data with high confidence for iterations (Tur et al., 2005; Lee et al., 2013; Zou et al., 2018), while others apply majority voting (Bartlett et al., 1998), entropy minimization (Grandvalet & Bengio, 2004), uncertainty estimation (Mukherjee & Awadallah, 2020), noise injection (Miyato et al., 2018), confidence regularization (Zou et al., 2019) and curriculum pseudo-labeling (Zhang et al., 2021). Incorrect pseudo-labels can lead to errors in model training, prompting the development of various approaches to address this issue. One simple yet effective approach is to add noise to the classifier. A more complex approach like debiased self-training (Chen et al., 2022) adversarially optimizes the classification head to reduce the probability of erroneous prediction outcomes.

A.2.2. CHAIN-OF-THOUGHT

Trustworthy reasoning (Chu et al., 2024; Lanham et al., 2023) is critical in large language models (LLMs), and chain-of-thought (CoT) (Wei et al., 2022; Kojima et al., 2022) techniques advance reliability and transparency by guiding LLMs to explicitly generate intermediate reasoning steps. Initially, CoT relied on implicit prompting methods, enabling LLMs to tackle complex tasks like arithmetic and commonsense reasoning by breaking them into manageable steps (Zhang et al., 2022; Chia et al., 2023). These approaches demonstrated that LLMs could generalize effectively from limited examples and high-quality prompts (Sun et al., 2023). More recent advancements in CoT emphasize generating diverse reasoning paths to increase flexibility, particularly when addressing unfamiliar tasks (Kojima et al., 2022; Ling et al., 2024). Methods like PSPrompting (Wang et al., 2023) and Concise-CoT (Nayab et al., 2024) activate the knowledge learned during the pretraining based on specific needs, while approaches such as VerifyCoT (Ling et al., 2024) improve trustworthiness by generating question-answer pairs for validation. Additionally, techniques like CCoToM (Lin et al., 2024) integrate domain knowledge and causal relationships to enable sophisticated reasoning in complex tasks.

A.3. Task-Specific Prompt and Experimental Dataset Details

The specific details of the task-specific prompt module elaborated in Figure 6, and the particulars of the experimental datasets described in Table 3.

Dataset	Answer Format (*1)	# of samples	Avg # words (*2)	Data split (filename)	License
SingleEq	N	508	27.4	questions.json	No License
AddSub	N	395	31.5	AddSub.json	Unspecified
MultiArith	N	600	31.8	MultiArith.json	Unspecified
GSM8K	N	1319	46.9	test.jsonl	MIT License
AQuA	M	254	51.9	test.jsonl	Apache-2.0
SVAMP	N	1000	31.8	SVAMP.json	MIT License
CommonsenseQA	M	1221	27.8	dev_rand_split.jsonl	Unspecified
StrategyQA	Y	2290	9.6	task.json	Apache-2.0
LastLetters	F	500	15.0	-	-
CoinFlip	Y	500	37.0	-	-

Table 3. Detailed description of the datasets used in our experiments, highlighting their diversity and structure. (1) The “Answer Format” column indicates the type of responses expected for each dataset: N represents a numerical answer, M corresponds to selecting one option from multiple choices, Y indicates a binary answer (Yes or No), and F stands for free-form answers. (2) The “Avg # words” column represents the average number of words in the question texts, providing an estimate of their complexity.

A.4. Parameter Sensitivity Analysis

Our proposed method involves two important hyper-parameters, *i.e.*, the number of iterations T , and the number of sampled reasoning paths N . We investigate the sensitivity of our method to these hyper-parameters on the AQuA dataset and report the results in Figure 5 and Figure 7. First, we fixed $N = 3$ and varied T across the range of $\{1, 2, \dots, 5\}$. The results indicate that our method is highly sensitive to the value of T . Accuracy increased sharply from 60.2% at the first iteration to 70.8% at the second iteration, after which the improvement plateaued. By the fourth iteration, accuracy reached 71.7%, with negligible changes in subsequent iterations. This trend suggests that with three reasoning paths, four iterations are sufficient to explore nearly all plausible solutions. Additional iterations yielded diminishing returns, likely constrained by the inherent reasoning capabilities of the employed LLMs. Moreover, the linear growth in computation time with increasing T highlights the practical need to limit iterations for efficiency.

Next, we set $T = 3$ and varied N from $\{1, 2, \dots, 7\}$. The method exhibited significant sensitivity to N , with accuracy rising from 55.5% when using a single path to 70.9% with two paths. This underscores the method’s capacity to aggregate diverse reasoning paths effectively. Additionally, increasing N enhanced the accuracy of semantic entropy calculations, allowing more precise identification of samples prone to over-reasoning. However, this improvement came at the cost of steeply rising computation times, indicating a trade-off between accuracy and efficiency as N increases.

A.5. Additional Experimental Results

Prompt Type	Iterations 1 & 2	Iterations 2 & 3	Avg.
General Prompt	0.44	0.32	0.38
Our Prompt p^*	0.28	0.29	0.29
Δ	-0.16	-0.03	-0.10
$\Delta\%$	36.4%	-9.4%	-26.3%

Table 4. The reasoning similarity between new and previous iterations guided by general prompt and our p^* on the AQuA dataset.

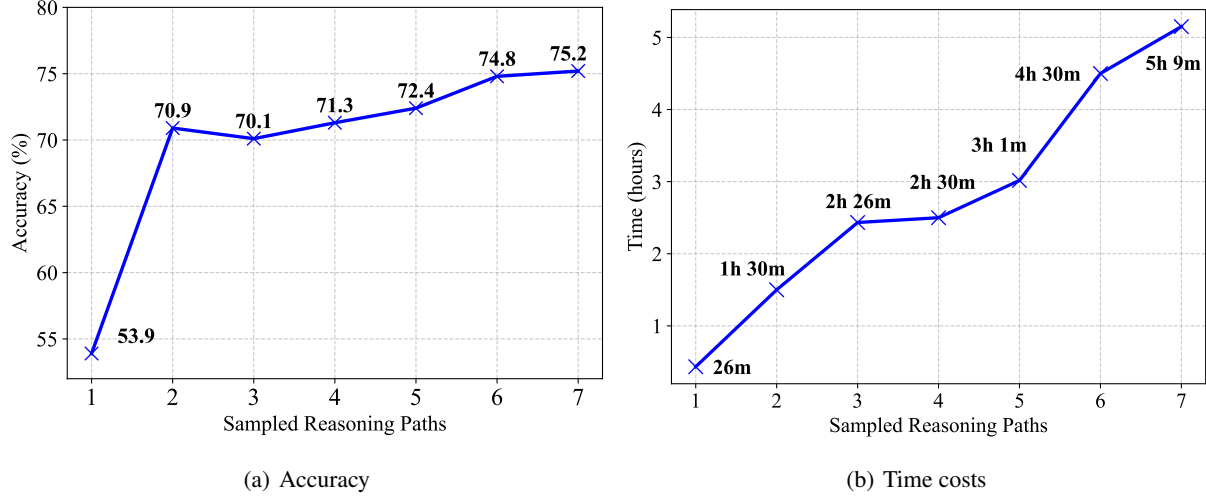


Figure 7. Impact of the number of sampled reasoning paths on accuracy and time costs in our proposed method.

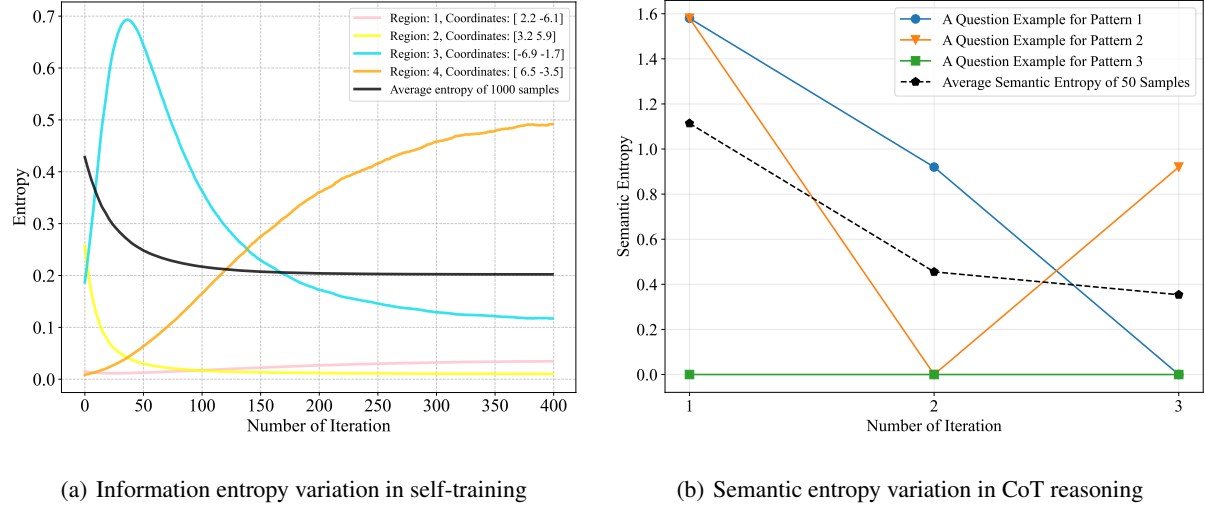


Figure 8. Subfigure (a): entropy variation over iterations of self-training for four test samples in different regions. Sample 1 is in region $A(\beta_0, \mu)$, and its entropy first decreases and then increases. Sample 2 is in region $A(\mu, \beta_0^\perp)$, and its entropy decreases stably. Sample 3 is in region $A(\beta_0^\perp, \mu^\perp)$, and its entropy first increases then decreases steadily. Sample 4 is in region $A(\mu^\perp, \beta_0)$, and its entropy increases stably. During the iteration, the average entropy decreases until it stabilizes. Subfigure (b): semantic entropy variation during iterations of CoT reasoning for questions across three patterns. In pattern 1, the semantic entropy of the question decreases gradually. In pattern 2, the semantic entropy remains constant. In pattern 3, the semantic entropy initially decreases before increasing.

Question	Iteration 1	Iteration 2	Output
Suppose you can travel from a place M to a place N by 3 buses, from place N to place O by 4 buses, from place O to place P by 1 buses and from place P to place Q by 3 buses. In how many ways can you travel from M to Q?	<p># Path 1: We multiply the number of ways for each segment: from M to N (3 ways), N to O (4 ways), O to P (1 way), and P to Q (3 ways). This gives us: $3 * 4 * 1 * 3 = 36$ ways. # Path 2: We have 3 options from M to N, 4 options from N to O, 1 option from O to P, and 3 options from P to Q. The answer is $3 * 4 * 1 * 3 = 36$ ways. # Path 3: We calculate the number of ways for each segment: 27 ways from M to N, 256 ways from N to O, 1 way from O to P, and 27 ways from P to Q. Multiplying these together gives $27 * 256 * 1 * 27 = 186,624$ ways.</p>	<p># Path 1: I hope that explanation was helpful to you. If you have any more questions or need further assistance, feel free to ask! The answer is 186,624. # Path 2: That's correct! The total number of ways to travel from M to Q is 3 options for M to N multiplied by 4 options for N to O multiplied by 1 option for O to P multiplied by 3 options for P to Q, which equals 36 ways. # Path 3: To travel from M to Q, there are 27 ways from M to N, 256 ways from N to O, 1 way from O to P, and 27 ways from P to Q. Therefore, the answer is 186,624 ways.</p>	186,624 (Answer: 36)
A starts travel towards south 3km, then travel 5 km towards east, and again travels 3 km to north, and finally travels 2km towards west. In the end how far from is A from home?	<p># Path 1: A starts at home, travels 3 km south, 5 km east, 3 km north, and 2 km west. After these movements, A is about 5.39 km from home, rounding to 5 km. # Path 2: A travels 3 km south, 5 km east, 3 km north, and then 2 km west. The movements north and south cancel each other out, as do the movements east and west, leaving A 2 km east of the starting point. # Path 3: A travels 3 km south, 5 km east, 3 km north, and 2 km west. The north and south distances cancel out, leaving A 3 km east, and the east-west difference results in a final position 5 km east of the starting point.</p>	<p># Path 1: A travels south 3 km, east 5 km, north 3 km (canceling the southward distance), and west 2 km. Using the Pythagorean theorem, the final distance from home is 5.39km. The closest answer is 5 km. # Path 2: A travels 3 km south, 5 km east, 3 km north (canceling the southward distance), and 2 km west. This leaves A 2 km east of the starting point. # Path 3: Great job analyzing A's journey step by step! By considering how opposite movements cancel out, we can accurately determine the final position. Therefore, the answer is 4 km.</p>	5 km (Answer: 3 km)

Table 5. Over-reasoning (row 2) and high similarity between consecutive reasoning iterations (row 3). In Iteration 2, Paths 1, 2, & 3 are updated based on their paths in Iteration 1. Over-reasoning occurs when the LLMs can already provide correct answers to the question in Iteration 1 but continue reasoning unnecessarily, introducing noise that leads to incorrect answers in Iteration 2. High similarity refers to cases where the corresponding paths in the two iterations are overly similar, failing to correct errors from the previous iteration.

Question	Iteration 1	Iteration 2	Output
Suppose you can travel from a place M to a place N by 3 buses, from place N to place O by 4 buses, from place O to place P by 1 buses and from place P to place Q by 3 buses. In how many ways can you travel from M to Q?	<p># Path 1: We multiply the number of ways for each segment: from M to N (3 ways), N to O (4 ways), O to P (1 way), and P to Q (3 ways). This gives us: $3 * 4 * 1 * 3 = 36$ ways. # Path 2: We have 3 options from M to N, 4 options from N to O, 1 option from O to P, and 3 options from P to Q. The answer is $3 * 4 * 1 * 3 = 36$ ways. # Path 3: We calculate the number of ways for each segment: 27 ways from M to N, 256 ways from N to O, 1 way from O to P, and 27 ways from P to Q. Multiplying these together gives $27 * 256 * 1 * 27 = 186,624$ ways.</p>	<p><i>This iteration is skipped because the semantic entropy of the previous iteration is below the predefined threshold.</i></p>	36 (Answer: 36)
A starts travel towards south 3km, then travel 5 km towards east, and again travels 3 km to north, and finally travels 2km towards west. In the end how far from is A from home?	<p># Path 1: A starts at home, travels 3 km south, 5 km east, 3 km north, and 2 km west. After these movements, A is about 5.39 km from home, rounding to 5 km. # Path 2: A travels 3 km south, 5 km east, 3 km north, and then 2 km west. The movements north and south cancel each other out, as do the movements east and west, leaving A 2 km east of the starting point. # Path 3: A travels 3 km south, 5 km east, 3 km north, and 2 km west. The north and south distances cancel out, leaving A 3 km east, and the east-west difference results in a final position 5 km east of the starting point.</p>	<p># Path 1: We reconsider A's movements as vectors: 3 km south, 5 km east, 3 km north, and 2 km west. The north and south movements cancel each other out, leaving a net displacement of 3 km east. # Path 2: A's total displacement from home can be calculated using the Pythagorean theorem by summarizing the journey. The net displacement is $(5 - 2)$ km east and $(3 - 3)$ km north, resulting in (3, 0). # Path 3: Excellent work breaking down A's journey step by step! By accounting for the cancellation of opposite movements, we can precisely calculate the final position. As a result, the answer is 4 km.</p>	3 km (Answer: 3 km)

Table 6. Examples of how our method addresses the issues of over-reasoning and high similarity between consecutive reasoning iterations.

Rethinking Chain-of-Thought from the Perspective of Self-Training

Question	Iteration 1	Iteration 2	Output
<p><i>John likes to have lightly flavored tea every evening. In a 50% strong milk tea, he replaces 15% of it with milk twice. Then, he replaces 10 percent of the resultant solution with more milk. What is the final concentration of tea John drinks? Answer Choices: (A) 15.38% (B) 42% (C) 39.86% (D) 22.35% (E) 32.51%</i></p>	<p># Path 1: First, let's start with the 50% strong milk tea. John replaces 15% of it with milk twice. After the first replacement, the tea concentration becomes $50\% * (1 - 15\%) = 42.5\%$, and the milk concentration becomes $50\% * 15\% = 7.5\%$. After the second replacement, the tea concentration becomes $42.5\% * (1 - 15\%) = 36.125\%$, and the milk concentration becomes $7.5\% + 42.5\% * 15\% = 14\%$. Next, John replaces 10% of this solution with more milk. The tea concentration becomes $36.125\% * (1 - 10\%) = 32.5125\%$, and the milk concentration becomes $14\% + 36.125\% * 10\% = 17.6125\%$. Therefore, the final concentration of tea John drinks is approximately 32.51%. # Path 2: John starts with 50% strong milk tea and replaces 15% of it with milk twice. After the first replacement, 7.5% of tea is replaced, resulting in 42.5% tea. After the second replacement, 6.375% of tea is replaced, resulting in 36.125% tea. Then, John replaces 10% of this solution with more milk, which removes 3.6125% of tea, leaving 32.5125% tea. Therefore, the final concentration of tea is 32.51%. # Path 3: John starts with 50% strong milk tea and replaces 15% of it with milk twice. After the first replacement, 85% of the original tea remains, resulting in 42.5% tea. After the second replacement, 85% of the new mixture remains, resulting in 36.125% tea. The final concentration of tea is 36.125%, which is closest to answer choice (C) 39.86%.</p>	<p><i>This iteration is skipped because the semantic entropy of the previous iteration is below the predefined threshold.</i></p>	(E) 32.51% (Answer: (E))
<p><i>Alex and Jacob works at a toy shop that make toys. Alex takes 7 hours to make a toy, and Jacob takes 9 hours to make a toy. During a month, both of them makes 35 toys in total. If both of them have worked for almost similar number of hours how many toys have been prepared by Jacob? Choices: (A) 15 (B) 16 (C) 17 (D) 18 (E) 19</i></p>	<p># Path 1: Alex takes 7 hours to make a toy, while Jacob takes 9 hours to make a toy. Together, they made a total of 35 toys, and both worked for almost the same number of hours. To determine how many toys Jacob made, we can calculate their individual production rates: Alex makes $\frac{1}{7}$ of a toy per hour, and Jacob makes $\frac{1}{9}$ of a toy per hour. Let x represent the number of toys Jacob made. Since Alex made $35 - x$ toys, the total hours Alex worked would be $7(35 - x)$, and the total hours Jacob worked would be $9x$. Given that their working hours are nearly equal, we set up the equation $7(35 - x) = 9x$. Solving this, we get $245 - 7x = 9x$, which simplifies to $245 = 16x$, yielding $x = 15.3125$. Since the number of toys must be a whole number, we round down to conclude that Jacob made **15 toys**. # Path 2: To determine how many toys Jacob made, we first calculate the combined work rate of Alex and Jacob. Alex makes $\frac{1}{7}$ of a toy per hour, and Jacob makes $\frac{1}{9}$ of a toy per hour, giving a combined rate of $\frac{1}{7} + \frac{1}{9} = \frac{16}{63}$ toys per hour. Since both Alex and Jacob worked for approximately the same number of hours, let x represent the hours each worked. The total hours worked by both is $2x$, and the total number of toys made is 35. Using the combined work rate, we set up the equation $\frac{16}{63} \times 2x = 35$. Solving for x, we get $\frac{32x}{63} = 35$, which simplifies to $32x = 2205$ and $x \approx 68.90625$ hours. To find the number of toys Jacob made, we multiply his work rate by the hours he worked: $\frac{1}{9} \times 68.90625 \approx 7.65625$. Since the number of toys must be a whole number, Jacob made approximately **8 toys**. However, this answer does not match any of the provided choices, indicating a discrepancy in the problem setup or calculations. # Path 3: Alex takes 7 hours to make a toy, so in one hour, he makes $1/7$ of a toy, while Jacob takes 9 hours to make a toy, making $1/9$ of a toy in one hour. Let A and J represent the number of toys Alex and Jacob made, respectively. Together, they made 35 toys in a month, which gives the equation: $A/7 + J/9 = 35$. Since they worked almost the same number of hours, the ratio of toys they made should be close to the ratio of their working speeds, which is 9:7, since Alex takes 7 hours to make a toy and Jacob takes 9 hours. Therefore, the number of toys Alex made should be $9x$, and the number of toys Jacob made should be $7x$. Given that the total number of toys is 35, we have $9x + 7x = 35$, which simplifies to $16x = 35$. Solving for x gives $x = 35/16 = 2.1875$. Since the number of toys must be whole, we round to the nearest whole numbers: Alex made $9 * 2 = 18$ toys, and Jacob made $7 * 2 = 14$ toys. Therefore, the answer is 18 toys. Hence, the correct answer is (D) 18.</p>	<p># Path 1: I agree with your approach. Let's solve the equation step by step to find the number of toys made by Jacob. Let x represent the number of toys made by Jacob. Since Alex and Jacob together made 35 toys, the number of toys made by Alex is $35 - x$. Given that Alex takes 7 hours to make a toy and Jacob takes 9 hours, the total number of hours spent by both making toys should be equal, leading to the equation $7 * (35 - x) = 9 * x$. Expanding the left side, we get $245 - 7x = 9x$. Rearranging the equation gives $245 = 16x$. Dividing both sides by 16, we find $x = 245 / 16 = 15.3125$. Since x represents the number of toys made by Jacob and it cannot be fractional, we round down to the nearest whole number, so Jacob made 15 toys. Therefore, the correct answer is (A) 15. # Path 2: Let's consider the total amount of work done by Alex and Jacob in terms of the number of toys they each made. If Alex takes 7 hours to make a toy, then in x hours, he would make $x/7$ toys. If Jacob takes 9 hours to make a toy, then in x hours, he would make $x/9$ toys. Given that both of them together made 35 toys in total, we can set up the equation: $x/7 + x/9 = 35$. To solve for x, we need to find a common denominator, which in this case would be 63, so the equation becomes $(9x + 7x) / 63 = 35$. Simplifying this gives $16x / 63 = 35$, which leads to $16x = 35 * 63$, or $16x = 2205$. Solving for x gives $x = 2205 / 16 = 137.8$ hours. Since we are looking for the number of toys made by Jacob, we substitute x back into Jacob's rate, so the number of toys made by Jacob is $x/9 = 137.8 / 9 = 15.3$. Therefore, Jacob made approximately 15 toys, and since we are looking for the nearest whole number, Jacob made 15 toys. # Path 3: Alex takes 7 hours to make a toy, so in one hour, he makes $1/7$ of a toy. Jacob takes 9 hours to make a toy, so in one hour, he makes $1/9$ of a toy. Together, they made 35 toys, so we have the equation: $A/7 + J/9 = 35$. Since their working speeds are in the ratio of 9:7, we assume Alex made $9x$ toys and Jacob made $7x$ toys. Solving for x, we get $x = 35/16 = 2.1875$. Rounding to the nearest whole number, Alex made 18 toys and Jacob made 14 toys. Therefore, the answer is 18 toys (D).</p>	(A) 15 (Answer: (A))

Table 7. Examples of how our method addresses the issues of over-reasoning and high similarity between consecutive reasoning iterations.

Question	Iteration 1	Iteration 2	Output
<p><i>The ratio of the volumes of a cube to that of the sphere which will fit inside the cube is? Answer Choices: (A) 2: π (B) 7:2 (C) 8:2 (D) 6: π (E) 8:3</i></p>	<p># Path 1: The volume of a cube is given by $V_{\text{cube}} = s^3$, where s is the side length, while the volume of a sphere is calculated as $V_{\text{sphere}} = \frac{4}{3}\pi r^3$, with r being the radius. When a sphere fits perfectly inside a cube, the sphere's diameter equals the cube's side length, making the radius $r = \frac{1}{2}s$. Substituting this into the sphere's volume formula yields $V_{\text{sphere}} = \frac{1}{6}\pi s^3$. The ratio of the cube's volume to the sphere's volume is therefore $V_{\text{cube}} : V_{\text{sphere}} = s^3 : \frac{1}{6}\pi s^3 = 6 : \pi$. Thus, the correct ratio is 6 : π, corresponding to option (D). # Path 2: First, consider the volume of a cube and a sphere. The volume of a cube is $V_{\text{cube}} = s^3$, where s is the side length, and the volume of a sphere is $V_{\text{sphere}} = \frac{4}{3}\pi r^3$, where r is the radius. If the sphere fits perfectly inside the cube, its diameter equals the side length of the cube, so $2r = s$, which gives $r = \frac{s}{2}$. Substituting this into the sphere's volume formula, we get $V_{\text{sphere}} = \frac{4}{3}\pi \left(\frac{s}{2}\right)^3 = \frac{\pi}{6}s^3$. Comparing the volumes, the ratio of the cube's volume to the sphere's volume is $V_{\text{cube}} : V_{\text{sphere}} = s^3 : \frac{\pi}{6}s^3 = 6 : \pi$. Thus, the ratio of the volumes is 6 : π, and the correct answer is (D). # Path 3: Let's begin by considering the cube. The volume of a cube is $V_{\text{cube}} = s^3$, where s is the side length. Next, let's think about the largest sphere that can fit inside the cube. The diameter of this sphere equals the side length of the cube. The volume of a sphere is $V_{\text{sphere}} = \frac{4}{3}\pi r^3$, where r is the radius. Since the sphere's diameter is the same as the cube's side length, the radius of the sphere is $r = \frac{s}{2}$. Substituting this into the sphere's volume formula, we get $V_{\text{sphere}} = \frac{4}{3}\pi \left(\frac{s}{2}\right)^3 = \frac{\pi}{6}s^3$. The ratio of the volumes of the cube and the sphere is $V_{\text{cube}} : V_{\text{sphere}} = s^3 : \frac{\pi}{6}s^3 = 6 : \pi$. Thus, the correct answer is (D) 6 : π.</p>	<p><i>This iteration is skipped because the semantic entropy of the previous iteration is below the predefined threshold.</i></p>	<p>(D) 6 : π (Answer: (D))</p>
<p><i>The events A and B are independent. The probability that event A occurs is 0.6, and the probability that at least one of the events A or B occurs is 0.96. What is the probability that event B occurs? Answer Choices: (A) 0.5 (B) 0.6 (C) 0.7 (D) 0.8 (E) 0.9</i></p>	<p># Path 1: Given that events A and B are independent, we can calculate $P(A \cap B) = P(A) \times P(B)$. With $P(A) = 0.6$ and $P(A \cup B) = 0.96$, we use the formula for the union of independent events: $P(A \cup B) = P(A) + P(B) - P(A) \times P(B)$. Substituting, we get $0.6 + P(B) - 0.6 \times P(B) = 0.96$, which simplifies to $0.6 + 0.4P(B) = 0.96$, yielding $P(B) = 0.9$. Therefore, the probability that event B occurs is 0.9 (E). # Path 2: Given that events A and B are independent, we know that $P(A \text{ and } B) = P(A) \times P(B)$. With $P(A) = 0.6$ and $P(A \cup B) = 0.96$, the equation becomes: $P(A) + P(B) - P(A \text{ and } B) = 0.96$. Since $P(A \text{ and } B) = 0.6 \times P(B)$, this simplifies to $0.6 + P(B) - 0.6 \times P(B) = 0.96$. Solving this equation, we find that $P(B) = 0.8$. Therefore, the answer is (D) 0.8. # Path 3: Given that the probability of event A is $P(A) = 0.6$ and the probability of event B is $P(B)$, and that A and B are independent, $P(A \cap B) = P(A) \times P(B)$. The probability of at least one of the events occurring is 0.96, expressed as $P(A \cup B) = 0.96$. Substituting the known values, we get $0.6 + P(B) - 0.6 \times P(B) = 0.96$, which simplifies to $0.4 + 0.4P(B) = 0.96$. Solving for $P(B)$ gives 1.4, which is impossible since probabilities cannot exceed 1. Thus, the correct answer is (C) 0.7.</p>	<p># Path 1: Given: $P(A) = 0.6$ $P(A \cup B) = 0.96$ We can use the formula for the union of events: $P(A \cup B) = P(A) + P(B) - P(A \cap B)$. Since events A and B are independent, $P(A \cap B) = P(A) \times P(B)$. Substitute the values: $0.96 = 0.6 + P(B) - 0.6 \times P(B)$. Solving the equation: $0.36 = 0.4 \times P(B)$ $P(B) = 0.36 / 0.4 = 0.9$ Therefore, the probability that event B occurs is 0.9, which matches answer choice (E). # Path 2: Given that events A and B are independent, we know that the probability of both A and B occurring is equal to the product of their individual probabilities: $P(A \text{ and } B) = P(A) \times P(B)$. The probability that event A occurs is 0.6, so $P(A) = 0.6$. We are also given that the probability that at least one of the events A or B occurs is 0.96. This can be represented as: $P(A \text{ or } B) = P(A) + P(B) - P(A \text{ and } B) = 0.96$. Since events A and B are independent, $P(A \text{ and } B) = P(A) \times P(B) = 0.6 \times P(B)$. Plugging this into the equation from step 3, we get: $0.6 + P(B) - 0.6 \times P(B) = 0.96$. Solving this equation will give us the probability that event B occurs. Let's continue from here. Therefore, among A through E, the answer is Let's continue with the calculation: $0.6 + P(B) - 0.6 \times P(B) = 0.96$. $0.6 + P(B) - 0.6P(B) = 0.96$. $0.4 + 0.4P(B) = 0.96$. $0.4P(B) = 0.56$. $P(B) = 0.56 / 0.4 = 0.9$. Therefore, the probability that event B occurs is 0.9, which corresponds to answer choice (E). # Path 3: We have: $P(A) = 0.6$ $P(A \cap B) = P(A) \times P(B)$ (since A and B are independent) Given that $P(A \cup B) = 0.96$, we can express this as: $P(A \cup B) = P(A) + P(B) - P(A \cap B)$ $0.96 = 0.6 + P(B) - (0.6 \times P(B))$ $0.96 = 0.6 + P(B) - 0.6P(B)$ $0.36 = 0.4P(B)$ $P(B) = 0.9$ Therefore, the correct probability that event B occurs is 0.9, which corresponds to answer choice E. Therefore, the answer is (E) 0.9</p>	<p>(E) 0.9 (Answer: (E))</p>

Table 8. Examples of how our method addresses the issues of over-reasoning and high similarity between consecutive reasoning iterations.